



# Lithium ameliorates rat spinal cord injury by suppressing glycogen synthase kinase-3 $\beta$ and activating heme oxygenase-1

Yonghoon Kim<sup>1,2</sup>, Jeongtae Kim<sup>1</sup>, Meejung Ahn<sup>1</sup>, Taekyun Shin<sup>1</sup>

<sup>1</sup>Department of Veterinary Anatomy, College of Veterinary Medicine, Jeju National University, Jeju, <sup>2</sup>HAEMALGEUN Veterinary Medical Clinic, Jeju, Korea

**Abstract:** Glycogen synthase kinase (GSK)-3 $\beta$  and related enzymes are associated with various forms of neuroinflammation, including spinal cord injury (SCI). Our aim was to evaluate whether lithium, a non-selective inhibitor of GSK-3 $\beta$ , ameliorated SCI progression, and also to analyze whether lithium affected the expression levels of two representative GSK-3 $\beta$ -associated molecules, nuclear factor erythroid 2-related factor-2 (Nrf-2) and heme oxygenase-1 (HO-1) (a target gene of Nrf-2). Intraperitoneal lithium chloride (80 mg/kg/day for 3 days) significantly improved locomotor function at 8 days post-injury (DPI); this was maintained until 14 DPI ( $P < 0.05$ ). Western blotting showed significantly increased phosphorylation of GSK-3 $\beta$  (Ser9), Nrf-2, and the Nrf-2 target HO-1 in the spinal cords of lithium-treated animals. Fewer neuropathological changes (e.g., hemorrhage, inflammatory cell infiltration, and tissue loss) were observed in the spinal cords of the lithium-treated group compared with the vehicle-treated group. Microglial activation (evaluated by measuring the immunoreactivity of ionized calcium-binding protein-1) was also significantly reduced in the lithium-treated group. These findings suggest that GSK-3 $\beta$  becomes activated after SCI, and that a non-specific enzyme inhibitor, lithium, ameliorates rat SCI by increasing phosphorylation of GSK-3 $\beta$  and the associated molecules Nrf-2 and HO-1.

**Key words:** Spinal cord injuries, Lithium, Glycogen synthase kinase-3 $\beta$ , NF-E2-related factor-2, Heme oxygenase-1

Received May 24, 2017; Revised July 18, 2017; Accepted July 24, 2017

## Introduction

Spinal cord injury (SCI) is characterized by both mechanical and inflammatory response-induced damage [1, 2]. The mechanical forces that impact the spinal cord at the time of

injury may cause immediate tissue bursting [3]. There are a variety of animal models of spinal cord injury, including those using weight-drop impact devices [4], the transection method [5], and clip-compression injuries [6-8]. Clip compression, which results in the progressive recovery of hindlimb paralysis in rats [9], is regarded as a manual injury technique for spinal cords in the absence of digital analysis systems, such as the Multicenter Animal Spinal Cord Injury Study (MASCIS) impactor [10]. The neuropathological features of SCI include edema, axonal degeneration, inflammatory cell infiltration, and exudation of fibronectin through the damaged blood-brain barrier [1, 4]. Activated neutrophils, microglia, and macrophages synthesize free radicals that trigger apoptosis of neurons and glia by irreversibly oxidizing polyunsaturated fatty acids, proteins, and DNA [5]. An increase in the cellular

### Corresponding authors:

Taekyun Shin

Department of Veterinary Anatomy, College of Veterinary Medicine, Jeju National University, 102 Jejudaehak-ro, Jeju 63243, Korea  
Tel: +82-64-754-3363, Fax: +82-64-756-3354, E-mail: shint@jejunu.ac.kr

Meejung Ahn

Department of Veterinary Anatomy, College of Veterinary Medicine, Jeju National University, 102 Jejudaehak-ro, Jeju 63243, Korea  
Tel: +82-64-754-3363, Fax: +82-64-756-3354, E-mail: healthy@jejunu.ac.kr

Copyright © 2017. Anatomy & Cell Biology

This is an Open Access article distributed under the terms of the Creative Commons Attribution Non-Commercial License (<http://creativecommons.org/licenses/by-nc/4.0/>) which permits unrestricted non-commercial use, distribution, and reproduction in any medium, provided the original work is properly cited.

antioxidant capacity or purging of reactive oxygen species (ROS) can protect against SCI.

Lithium, a non-selective inhibitor of glycogen synthase kinase (GSK)-3 $\beta$ , has been used as a mood stabilizer in patients with bipolar disorder, and possibly acts as a neuroprotectant [6]. Lithium has also been used to ameliorate chronic experimental autoimmune encephalomyelitis (EAE) in mice expressing anti-myelin oligodendrocyte glycoprotein antibodies [7], and acute monophasic EAE in the rat [8]. In addition, lithium is used to protect neurons after SCI, reducing post-injury inflammation [9]. Lithium promotes the production and release of neurotrophins, stimulates neurogenesis, enhances autophagy, and inhibits apoptosis [10]. However, any neuroprotective effect of lithium in terms of activating antioxidative systems, such as the nuclear factor erythroid 2-related factor 2 (Nrf-2)/heme oxygenase-1 (HO-1) mechanism requires further study in models of SCI.

Oxidative stress-induced cell damage is attributable to an imbalance between reactive oxygen free radical production and the efficacy of the anti-oxidant system [11]. An increase in cellular antioxidant capacity or ROS removal can ameliorate various diseases and injuries, including SCI [12]. Nrf-2 and its downstream target (HO-1), along with other antioxidant enzymes including superoxide dismutase and glutathione peroxidase play important roles in protecting various tissues and cells against oxidative stress both by regulating the expression levels of cytoprotective and antioxidant genes [12] and reducing inflammation [13]. Normally, Nrf-2 is associated with the Kelch like-ECH-associated protein 1 (Keap1) in the cytoplasm; upon stimulation, Nrf-2 is translocated to the nucleus where it plays essential roles in the transcription of various phase II and/or antioxidant enzyme genes [14]. Targeting of Nrf-2/HO-1 after SCI suppresses oxidative stress and exerts a neuroprotective effect [15]. However, any relationship between GSK-3 $\beta$  and Nrf-2 expression in the SCI rat model remains unclear.

In the present study, we investigated the neuroprotective effects of lithium, a non-selective inhibitor of GSK-3 $\beta$ , in rats where SCI was induced by clip compression. We explored the underlying protective molecular mechanisms via semi-quantitative analysis of Nrf-2 and HO-1 levels.

## Materials and Methods

### Animals

We used female Sprague-Dawley rats (200–250 g, 7–8

weeks of age) (OrientBio Inc., Seongnam, Korea). All experimental procedures were conducted in accordance with the Guidelines for the Care and Use of Laboratory Animals of Jeju National University. The animal protocols also conformed to current international laws and policies National Institutes of Health (NIH) Guide for the Care and Use of Laboratory Animals, NIH Publication No. 85-23, 1985, revised 1996. Every effort was made to minimize the number of animals used and their suffering.

### Surgical procedures

Clip compression injury was inflicted using a modification of previously published methods [1, 16, 17]. Animals were anesthetized via intramuscular injection of Zoletil 50 (Virbac, Carros, France) and subjected to laminectomy at T9/T10. Immediately thereafter, the spinal cord was compressed with a vascular clip (Stoelting, Wood Dale, IL, USA) applied vertically to the exposed spinal cord at an occlusion pressure of 15–20 g for 1 minute. After compression, the muscles and skin layers were closed. Sham-operated control rats underwent laminectomy only. Spinal cord tissues from the surgical sites were harvested and either fixed in 4% (v/v) paraformaldehyde in phosphate-buffered saline (PBS; pH 7.2) for histological examination or stored at –80°C prior to Western blot analysis.

### Antibodies

We used a rabbit anti-Iba-1 (Wako Pure Chemical Industries Ltd., Osaka, Japan) antibody to immunohistochemically stain the ramified microglia and macrophages of rat spinal cords, and for Western blotting. We employed monoclonal rabbit anti-phospho-GSK-3 $\beta$  (Ser9) (p-GSK-3 $\beta$ ) and monoclonal rabbit anti-GSK-3 $\beta$  antibodies (Cell Signaling Technology, Beverly, MA, USA) to detect GSK-3 $\beta$ . Rabbit polyclonal anti-Nrf-2 and -HO-1 antibodies (Santa Cruz Biotechnology, Santa Cruz, CA, USA) were used to stain the respective proteins. We also employed a mouse monoclonal anti- $\beta$ -actin antibody (Sigma-Aldrich, St. Louis, MO, USA).

### Lithium treatment

To assess the effects of lithium on SCI, rats were divided into the following three treatment groups (10 animals/group): sham control, vehicle, and lithium. To rapidly elevate the lithium level, the first dose of lithium chloride (80 mg/kg/day, Sigma-Aldrich) was intraperitoneally injected into the lithium-treated group 30 minutes after surgery; identical doses were given on each of the next 3 days. Lithium is nontoxic to rats at

this level; the serum levels are equivalent to those in human patients [7]. As in our previous study, serum lithium concentrations were measured using a lithium assay kit (catalog number LI01ME, MG Metallogenics, Chiba, Japan) [8]. The body weights and behavioral features of all rats were checked daily.

### **Behavioral tests and histological examination**

Locomotor function after SCI was examined using the Basso, Beattie, and Bresnahan (BBB) rating scale. All evaluations were performed in a double-blinded manner; average scores were calculated for each group and used to compare the severity of hind-limb paralysis.

Spinal cords collected at various time points (0, 4, 7, and 14 days post-injury [DPI]) were perfused with 4% (v/v) paraformaldehyde in PBS, pH 7.2. The T8–T10 regions of the spinal cords, including the sites of injury, were collected and post-fixed in 10% (v/v) neutral-buffered formalin for 48 hours. Subsequently, sagittal sections (5  $\mu$ m thick) were stained with hematoxylin and eosin.

### **Immunohistochemistry**

To assess early responses to treatment, we compared the microglial features of the vehicle- and lithium-treated groups at 4 DPI, as microglial reactions are prominent within the first week after SCI [18–20]. We immunostained the spinal cord for Iba-1 (a marker of activated cord microglia and macrophages) as described previously [13]. Briefly, after incubation with matched blocking serum (10% [v/v] normal goat serum in PBS, Vectastain Elite ABC kit, Vector Laboratories, Burlingame, CA, USA), the samples were incubated with rabbit anti-Iba-1 (Iba-1, 1:800, Wako Pure Chemical Industries Ltd.) for 1 hour at room temperature. After three washes in PBS, we proceeded as recommended by the manufacturer; the peroxidase reaction was developed using a diaminobenzidine substrate kit (Vector Laboratories).

### **Western blot analysis**

We performed Western blotting as described previously [21]. Briefly, spinal cord tissue was homogenized in TNN lysis buffer containing protease and phosphatase inhibitors (1 mM  $\text{Na}_3\text{VO}_4$ , 1 mM phenylmethanesulphonylfluoride, 10  $\mu$ g/ml aprotinin, 10  $\mu$ g/ml leupeptin), centrifuged at 10,900  $\times$ g for 20 minutes at 4°C, and the supernatant was harvested. The cytosolic and nuclear fractions were separated using NE-PER Nuclear and cytoplasmic extraction reagents as recommend-

ed by the manufacturer (Thermo Scientific, Rockford, IL, USA). Proteins (40  $\mu$ g) were subjected to 10% (w/v) sodium dodecyl (or lauryl) sulfate polyacrylamide gel electrophoresis and transferred to nitrocellulose membranes (Schleicher and Schuell, Keene, NH, USA). The membranes were blocked by incubation with 5% (v/v) skim milk in Tris-buffered saline for 1 hour and then incubated with primary antibodies (anti-p-GSK-3 $\beta$ , 1:1,000 dilution; anti-GSK-3 $\beta$ , 1:1,000 dilution; anti-Nrf-2, 1:1,000 dilution; and anti-HO-1, 1:1,000 dilution) for 2 hours. After washing, the membranes were incubated with the appropriate secondary antibodies for 1 hour. Bound antibodies were detected using a chemiluminescent substrate (in the WEST-one kit, iNtRON Biotech, Seongnam, Korea) according to the manufacturer's instructions. After imaging, the membranes were stripped and reprobed using an anti- $\beta$ -actin antibody (1:10,000 dilution). The optical density (OD)/mm<sup>2</sup> of each band was measured using ImageJ software (NIH, Bethesda, MD, USA). To detect Iba-1, we used the Wes system (ProteinSimple, San Jose, CA, USA) as instructed by the simple western user manual [22]. All electrophoresis and immunoblotting steps were performed using a fully automated capillary system.

### **Statistical analysis**

All measurements are averages of three independent experiments. All values are presented as means $\pm$ standard error of the mean. The results were analyzed using a one-way analysis of variance (ANOVA) followed by Student-Newman-Keuls *post hoc* testing for multiple comparisons. A *P*-value of < 0.05 was considered to reflect statistical significance.

## **Results**

### **Lithium-mediated behavioral changes**

Locomotor function began to recover commencing on 3 DPI. By 8 DPI, the BBB scores was significantly higher in the lithium-treated group (10.4 $\pm$ 0.52, *P*<0.05) compared with those of the vehicle-treated group (6.78 $\pm$ 0.55); the improvements were maintained until 14 DPI (Fig. 1).

### **Histological findings**

The sham-operated group exhibited no mechanical change in the core region of the spinal cord (data not shown), as found previously [1, 17]. The cords of vehicle-treated rats exhibited reduced cellularity and edema in longitudinal sections of core lesions (Fig. 1A). Inflammatory cells had infiltrated by



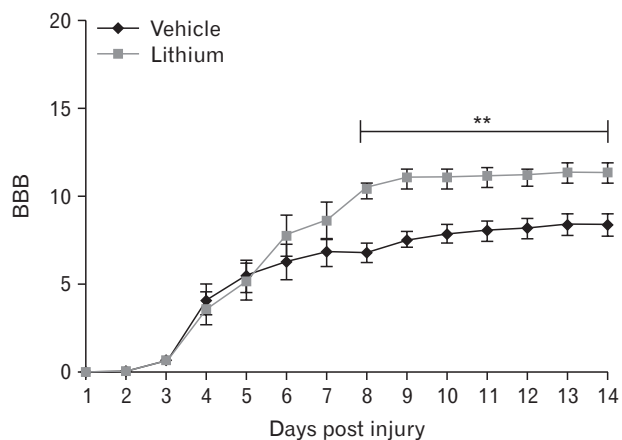


Fig. 1. Locomotor outcomes as evaluated by Basso, Beattie, and Bresnahan (BBB) scoring ( $n=5$ /daily). The BBB scores were very low in both groups to 3 days post-injury; on day 8 post-injury, the BBB score in the lithium-treated group was significantly higher than that in the vehicle-treated group. This difference persisted until 14 days post-injury.  $**P<0.01$  vs. vehicle-treated group.

4 DPI (Fig. 2C). In contrast, severe edema and hemorrhage were evident in the lithium-treated group (Fig. 2B). Additionally, accumulation of round-type inflammatory cells (Fig. 2D); activated microglia; and small, round vacuoles were evident in the core regions of spinal cords of the lithium-treated group by 4 DPI (Fig. 2D).

### Microglial reactions and infiltration of inflammatory cells

To assess microglial reactions and inflammatory cell infiltration, we immunohistochemically stained for Iba-1 and used a simple system to quantify the protein levels. Iba-1-positive microglial cells and macrophages were evident in all cord regions, including the white and gray matter (Fig. 3). Fig. 3C illustrates a representative experiment; the data are displayed in pseudo-gel and electropherogram formats. By 4 DPI, the Iba-1 level in the lithium-treated group ( $25.78\pm9.99\%$ , rela-

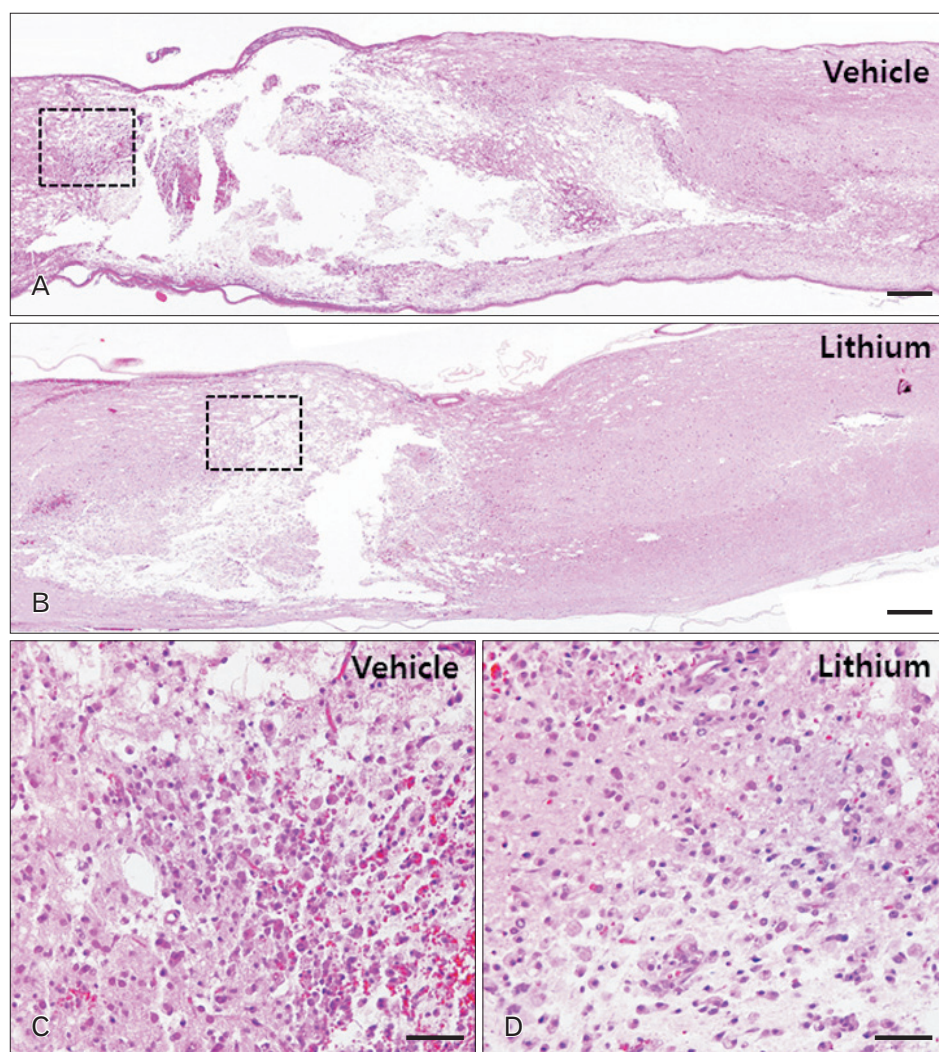


Fig. 2. Histological profiles of the spinal cords of vehicle-treated (A, C) and lithium-treated groups (B, D) 4 days post-injury. (A, B) Low-magnification images of sagittal sections. (C, D) High-magnification images of the squares in panels (A) and (B), respectively. A–D, hematoxylin and eosin staining. Scale bars = 100  $\mu$ m (A, B), 20  $\mu$ m (C, D).

tive OD) was significantly less than that in the vehicle-treated group ( $50.93 \pm 6.39\%$ , relative OD;  $P < 0.05$ ) (Fig. 3C).

### Lithium-mediated modulation of the levels of GSK-3 $\beta$ , Nrf-2, and HO-1 in the spinal cords of injured rats

We evaluated the GSK-3 $\beta$  phosphorylation status via Western blotting to explore whether lithium inhibited GSK-

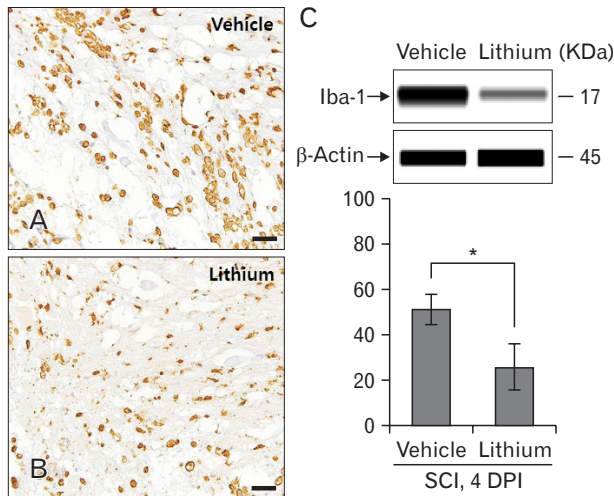


Fig. 3. Ionized calcium-binding protein 1 (Iba-1) immunostaining of the core cord regions of vehicle-treated (A) and lithium-treated groups (B) on day 4 post-injury. Iba-1-positive microglial cells were evident in all regions, including the white and gray matter. Ramified microglial cells and many inflammatory cells immunostained for Iba-1 in the core cord regions of both groups. Scale bars=100  $\mu$ m (A, B). (C) Bar graphs: semi-quantitative analysis of Iba-1 levels (~17 kDa protein) using a simple Western blotting system. Normalization was achieved by reprobating the membranes with an anti- $\beta$ -actin antibody. Means $\pm$ SE (n=5 per group) are shown. \* $P < 0.05$  vs. the vehicle-treated group. SCI, spinal cord injury; DPI, days post-injury.

3 $\beta$  activity in the spinal cords of injured rats (n=5 per group). Lithium significantly increased the p-GSK-3 $\beta$  expression level (relative OD values,  $2.92 \pm 0.44$ -fold;  $P < 0.05$ ) compared with vehicle ( $1.00 \pm 0.13$ -fold) at 4 DPI (Fig. 4A). We performed

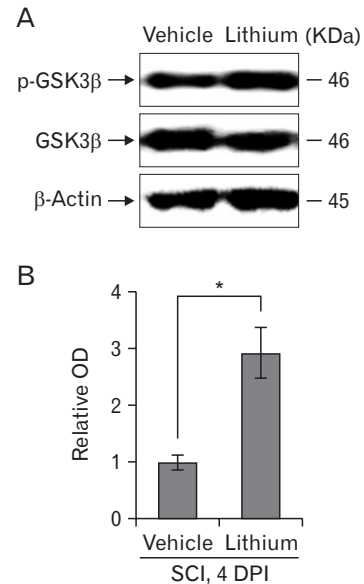


Fig. 4. Western blotting to detect glycogen synthase kinase (GSK)-3 $\beta$  in rats with spinal cord injury (SCI). (A) Representative immunoblots of phosphorylated GSK (p-GSK)-3 $\beta$  (Ser9), total GSK-3 $\beta$  (~46 kDa), and  $\beta$ -actin (~45 kDa). (B) The p-GSK-3 $\beta$  level increased significantly in the spinal cords of lithium-treated rats. To quantify GSK-3 $\beta$  phosphorylation, the levels of the phosphorylated form were normalized to those of total GSK-3 $\beta$ . Normalization was achieved by reprobating the membranes with an anti- $\beta$ -actin antibody. Means $\pm$ SEM (n=5 per group) are shown. \* $P < 0.05$  vs. the lithium-treated group. DPI, days post-injury.

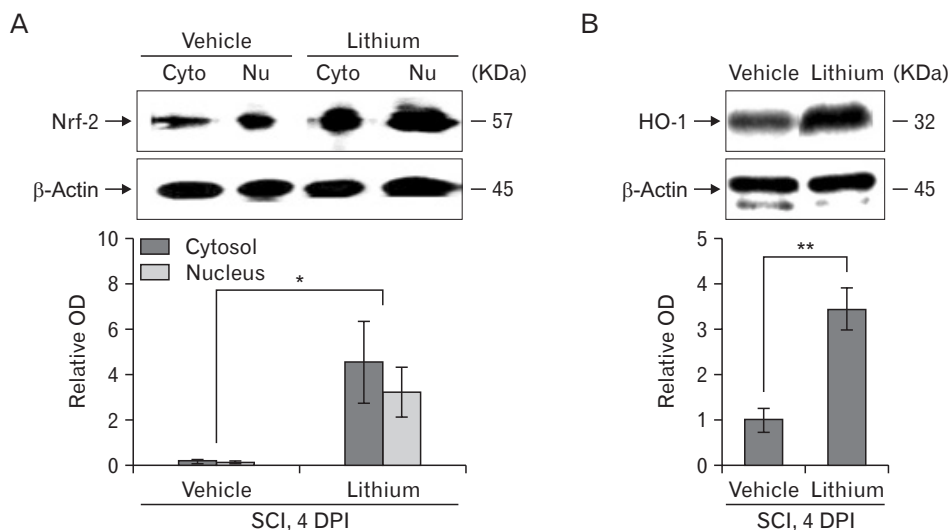


Fig. 5. Western blotting to detect nuclear factor erythroid 2-related factor-2 (Nrf-2) and heme oxygenase-1 (HO-1) in the spinal cords of rats with spinal cord injury (SCI). (A, B) Representative immunoblots of Nrf-2 (~57 kDa), HO-1 (~32 kDa), and  $\beta$ -actin (~45 kDa). Bar graphs: Both the Nrf-2 and HO-1 levels increased significantly and Nrf-2 was translocated from the cytoplasm to the nucleus in the spinal cords of lithium-treated rats. Normalization was achieved by reprobating the membranes with an anti- $\beta$ -actin antibody. Means $\pm$ SEM (n=5 per group) are shown. \* $P < 0.05$ , \*\* $P < 0.01$  vs. the lithium-treated group. Cyto, cytoplasm; Nu, nucleus; OD, optical density; DPI, days post-injury.

Western blotting to determine whether lithium influenced Nrf-2 levels in the cytosol and nucleus. Lithium significantly increased both the cytoplasmic Nrf-2 level ( $4.54 \pm 1.76$ -fold, relative OD/mm<sup>2</sup>,  $P < 0.05$ ) compared with the vehicle-treated group ( $0.21 \pm 0.04$ -fold) and also the extent of nuclear translocation ( $3.23 \pm 1.08$ -fold,  $P < 0.05$ ) compared with the vehicle-treated group ( $0.14 \pm 0.04$ -fold) (Fig. 5A). In addition, the HO-1 protein level in the lithium-treated group was significantly greater ( $3.42 \pm 0.46$ -fold,  $P < 0.01$ ) than that in the vehicle-treated group ( $1.00 \pm 0.26$ -fold) (Fig. 5B), reflecting enhanced Nrf-2 expression and translocation in SCI rats given lithium.

## Discussion

Many types of SCI models have been developed using rodents [4]. To obtain reliable data associated with impact power, computerized data analyses have been applied using the New York University impact device [23], Ohio State University impact device [18], and MASCIS impactor [19]. Alternatively, for the present study, a clip compression technique was employed to induce SCI because there is a progressive improvement in BBB scores in rats following the use of this technique [2, 21, 24]. Additionally, the clip compression technique is an alternative choice for the induction of SCI in the absence of digital analysis systems, such as MASCIS [23].

We first showed that lithium exerted significant anti-inflammatory and anti-oxidative effects by inhibiting inflammatory cell infiltration, microglial activation, and Nrf-2 translocation (thus enhancing HO-1 synthesis), significantly improving functional recovery in rats. Earlier, we showed that lithium treatment reduced the extent of the Iba-1-positive area of the spinal cord, and reduced the serum tumor necrosis factor  $\alpha$  level, in an experimental rat model of EAE [8]. Lithium suppresses both the level of circulating pro-inflammatory mediators and the number of central nervous system microglial cells, and enhances locomotor function in rats with SCI. A previous report indicated that GSK-3 $\beta$ , a negative regulator of Nrf-2, influenced the relative Nrf-2 proportions in the cytosol and nucleus [19]. Here, we show that lithium-mediated inhibition of GSK-3 $\beta$  induced nuclear Nrf-2 accumulation, thus activating HO-1, in rats with SCI.

Lithium chloride reduces the disruption in the blood-spinal cord barrier and promotes the recovery of neurological function after SCI. This occurs partly due to decreases in the activation of endoplasmic reticulum stress, which plays an

important role in SCI by inhibiting GSK-3 $\beta$  activation [20]. In the present study, lithium inhibited GSK-3 $\beta$  phosphorylation and thus may have reduced inflammation in the spinal cord samples subjected to clip compression. Additionally, the regulation of GSK-3 $\beta$  activity is generally mediated by phosphorylation of the amino-terminal domain (at Ser9) by any of several kinases, including Akt, protein kinase A, and/or protein kinase C, which inactivate the enzyme [21]. Furthermore, toll-like receptors mediate GSK-3 $\beta$  phosphorylation at Ser9 via the regulation of pro- and anti-inflammatory cytokines [22]. Thus, it is possible that the inhibition of GSK-3 $\beta$  relieves the clip compression SCI in rats.

Various drugs exert antioxidative neuroprotective activities in the spinal cord by activating Nrf-2 such as asiatic acid, rosmarinic acid and resveratrol [12, 25-27]. In Wistar rats, carnosol protects against SCI-induced oxidative stress and inflammation by modulating nuclear factor- $\kappa$ B, cyclooxygenase-2, and Nrf-2 levels [26]. Several drugs associated with Nrf-2 activation have been used to treat rat SCI; however, this is the first report to show that lithium-mediated inhibition of GSK-3 $\beta$  protects against SCI by regulating Nrf-2 translocation and subsequent activation of the HO-1 target gene. Recent evidence indicates that GSK-3 $\beta$  plays a critical role in regulating and degrading Nrf-2 in a Keap1-independent manner [28]. Furthermore, it was postulated that lithium exerts neuroprotective effects via the activation of Nrf-2 in spinal cord-injured rats.

In conclusion, our findings suggest that lithium ameliorates rat paralysis caused by SCI, and that the molecular mechanism involves inhibition of GSK-3 $\beta$ , increased nuclear translocation of Nrf-2, and subsequent upregulation of HO-1.

## Acknowledgements

This research was supported by the Basic Science Research Program of the National Research Foundation of Korea (NRF), funded by the Ministry of Education (Grant number: NRF-2014R1A1A2055965).

## References

1. Jung K, Min DS, Sim KB, Ahn M, Kim H, Cheong J, Shin T. Up-regulation of phospholipase D1 in the spinal cords of rats with clip compression injury. *Neurosci Lett* 2003;336:126-30.
2. Ahn M, Moon C, Park C, Kim J, Sim KB, Shin T. Transient activation of an adaptor protein, disabled-2, in rat spinal cord injury.



- Acta Histochem 2015;117:56-61.
3. Kwon BK, Tetzlaff W, Grauer JN, Beiner J, Vaccaro AR. Pathophysiology and pharmacologic treatment of acute spinal cord injury. *Spine J* 2004;4:451-64.
  4. Shin T, Ahn M, Moon C, Kim S, Sim KB. Alternatively activated macrophages in spinal cord injury and remission: another mechanism for repair? *Mol Neurobiol* 2013;47:1011-9.
  5. Donnelly DJ, Popovich PG. Inflammation and its role in neuroprotection, axonal regeneration and functional recovery after spinal cord injury. *Exp Neurol* 2008;209:378-88.
  6. Grimes CA, Jope RS. The multifaceted roles of glycogen synthase kinase 3beta in cellular signaling. *Prog Neurobiol* 2001;65:391-426.
  7. De Sarno P, Li X, Jope RS. Regulation of Akt and glycogen synthase kinase-3 beta phosphorylation by sodium valproate and lithium. *Neuropharmacology* 2002;43:1158-64.
  8. Ahn M, Kim J, Park C, Cho J, Jee Y, Jung K, Moon C, Shin T. Potential involvement of glycogen synthase kinase (GSK)-3beta in a rat model of multiple sclerosis: evidenced by lithium treatment. *Anat Cell Biol* 2017;50:48-59.
  9. Fang XY, Zhang WM, Zhang CF, Wong WM, Li W, Wu W, Lin JH. Lithium accelerates functional motor recovery by improving remyelination of regenerating axons following ventral root avulsion and reimplantation. *Neuroscience* 2016;329:213-25.
  10. Young W. Review of lithium effects on brain and blood. *Cell Transplant* 2009;18:951-75.
  11. Pratheeshkumar P, Son YO, Divya SP, Roy RV, Hitron JA, Wang L, Kim D, Dai J, Asha P, Zhang Z, Wang Y, Shi X. Luteolin inhibits Cr(VI)-induced malignant cell transformation of human lung epithelial cells by targeting ROS mediated multiple cell signaling pathways. *Toxicol Appl Pharmacol* 2014;281:230-41.
  12. Jiang W, Li M, He F, Bian Z, He Q, Wang X, Yao W, Zhu L. Neuroprotective effect of asiatic acid against spinal cord injury in rats. *Life Sci* 2016;157:45-51.
  13. Ahn M, Kim J, Bang H, Moon J, Kim GO, Shin T. Hepatoprotective effects of allyl isothiocyanate against carbon tetrachloride-induced hepatotoxicity in rat. *Chem Biol Interact* 2016;254:102-8.
  14. Chen XL, Dodd G, Thomas S, Zhang X, Wasserman MA, Rovin BH, Kunsch C. Activation of Nrf2/ARE pathway protects endothelial cells from oxidant injury and inhibits inflammatory gene expression. *Am J Physiol Heart Circ Physiol* 2006;290:H1862-70.
  15. Lv R, Mao N, Wu J, Lu C, Ding M, Gu X, Wu Y, Shi Z. Neuroprotective effect of allicin in a rat model of acute spinal cord injury. *Life Sci* 2015;143:114-23.
  16. Kim DH, Heo SD, Ahn MJ, Sim KB, Shin TK. Activation of embryonic intermediate filaments contributes to glial scar formation after spinal cord injury in rats. *J Vet Sci* 2003;4:109-12.
  17. Ahn M, Lee C, Jung K, Kim H, Moon C, Sim KB, Shin T. Immunohistochemical study of arginase-1 in the spinal cords of rats with clip compression injury. *Brain Res* 2012;1445:11-9.
  18. Koshinaga M, Whittemore SR. The temporal and spatial activation of microglia in fiber tracts undergoing anterograde and retrograde degeneration following spinal cord lesion. *J Neurotrauma* 1995;12:209-22.
  19. Dusart I, Schwab ME. Secondary cell death and the inflammatory reaction after dorsal hemisection of the rat spinal cord. *Eur J Neurosci* 1994;6:712-24.
  20. Loane DJ, Byrnes KR. Role of microglia in neurotrauma. *Neurotherapeutics* 2010;7:366-77.
  21. Kim H, Moon C, Ahn M, Byun J, Lee Y, Kim MD, Matsumoto Y, Koh CS, Shin T. Heat shock protein 27 upregulation and phosphorylation in rat experimental autoimmune encephalomyelitis. *Brain Res* 2009;1304:155-63.
  22. Chen JQ, Heldman MR, Herrmann MA, Keddi N, Woo W, Blumberg PM, Goldsmith PK. Absolute quantitation of endogenous proteins with precision and accuracy using a capillary Western system. *Anal Biochem* 2013;442:97-103.
  23. Vijayaprakash KM, Sridharan N. An experimental spinal cord injury rat model using customized impact device: a cost-effective approach. *J Pharmacol Pharmacother* 2013;4:211-3.
  24. Basso DM, Fisher LC, Anderson AJ, Jakeman LB, McTigue DM, Popovich PG. Basso Mouse Scale for locomotion detects differences in recovery after spinal cord injury in five common mouse strains. *J Neurotrauma* 2006;23:635-59.
  25. Shang AJ, Yang Y, Wang HY, Tao BZ, Wang J, Wang ZF, Zhou DB. Spinal cord injury effectively ameliorated by neuroprotective effects of rosmarinic acid. *Nutr Neurosci* 2017;20:172-9.
  26. Wang ZH, Xie YX, Zhang JW, Qiu XH, Cheng AB, Tian L, Ma BY, Hou YB. Carnosol protects against spinal cord injury through Nrf-2 upregulation. *J Recept Signal Transduct Res* 2016;36:72-8.
  27. Kesherwani V, Atif F, Yousuf S, Agrawal SK. Resveratrol protects spinal cord dorsal column from hypoxic injury by activating Nrf-2. *Neuroscience* 2013;241:80-8.
  28. Rada P, Rojo AI, Chowdhry S, McMahon M, Hayes JD, Cuadrado A. SCF/ $\beta$ -TrCP promotes glycogen synthase kinase 3-dependent degradation of the Nrf2 transcription factor in a Keap1-independent manner. *Mol Cell Biol* 2011;31:1121-33.